The Chlorination Kinetics of Tungsten, Molybdenum, and their Alloys

A. Landsberg, C. L. Hoatson and F. E. Block

J. Electrochem. Soc. 1971, Volume 118, Issue 8, Pages 1331-1336.
doi: 10.1149/1.2408316

Conclusions

1. Submicroscopic faceting of Cu surfaces occurs during gaseous pretreatment, having a major effect on subsequent oxidation rates. Electron micrographs confirm that faceting occurs and that it is a reversible process.

2. Gaseous pretreatment in H_2 favors facets of slowly oxidizing predominately (111) orientation, whereas in N_2, the effects of which are ascribed to traces of O_2, the rapidly oxidizing predominately (100) orientation is favored.

Activation energies (9700 cal/mole) for facet formation are in accord with a surface diffusion process.

3. Oxidation rates, according to oxide thickness measurements, decrease in the order: (100) > (111) > (110), but, according to activation energies, in the order: (100) > (110) > (111).

4. All three faces follow two-stage logarithmic kinetics at 175°, 200°, and 225°C. This is also true of treated (100) and (111) faces oxidized at 200°C.

5. Work functions calculated from activation energies of oxidation indicate that modification of the metal work function at the metal-oxide interface is orientation dependent.

Acknowledgment

The authors express their appreciation to the National Steel Company for financial support. They are grateful to John Breedis and Robert Goss for guidance in preparing the electron micrographs.

Manuscript submitted Nov. 4, 1970; revised manuscript received ca. March 20, 1971. This was Paper 98 presented at the Atlantic City Meeting of the Society, Oct. 4-8, 1970.

Any discussion of this paper will appear in a Discussion Section to be published in the June 1972 JOURNAL.

REFERENCES

1. A. Rönnquist and H. Fischmeister, *J. Inst. Metals*, **89**, 65 (1960-1961).
2. W. Bradley and H. Uhlig, *This Journal*, **114**, 669 (1967).
3. W. Campbell and U. Thomas, *Trans. Electrochem. Soc.*, **76**, 303 (1939).
4. B. Lustman and R. Mehl, *Trans. AIME.*, **143**, 246 (1941).
5. R. Tylecoat, *J. Inst. Metals*, **78**, 327 (1950).
6. Quoted by H. H. Uhlig, *Acta Met.*, **4**, 541 (1956).
7. V. Nwoko and H. Uhlig, *This Journal*, **112**, 1181 (1965).
8. H. Uhlig, J. Pickett, and J. MacNairn, *Acta Met.*, **7**, 111 (1959).
9. B. Lustman, *Trans. Electrochem. Soc.*, **81**, 359 (1942).
10. A. Gwathmey and A. Benton, *J. Phys. Chem.*, **46**, 969 (1942).
11. F. Young, J. Cathcart, and A. Gwathmey, *Acta Met.*, **4**, 145 (1956).
12. W. Harris, F. Ball, and A. Gwathmey, *ibid.*, **5**, 574 (1957).
13. S. Ali and G. Wood, *Corrosion Sci.*, **8**, 413 (1968).
14. C. Tucker, Jr., *Acta Met.*, **15**, 1465 (1967).
15. J. Moreau and J. Bénard, *Compt. Rend. Acad. Sci. Paris*, **242**, 1724 (1956).
16. G. Rhead, *Acta Met.*, **11**, 1035 (1963); **13**, 223 (1965); *Trans. Faraday Soc.*, **61**, 797 (1965).
17. F. Gronlund, *J. Chim. Phys.*, **53**, 660 (1956).
18. J. Bénard and J. Talbot, *Compt. Rend. Acad. Sci. Paris*, **225**, 411 (1947).
19. N. Underwood, *Phys. Rev.*, **47**, 502 (1935).
20. P. Köhler, *Z. Angew. Phys.*, **21**, 191 (1966).
21. J. Cathcart, G. Petersen, and C. Sparks, Jr., Proc. Nucléation Dans Les Réactions des Gaz Sur Les Métaux, p. 11, Centre National de La Recherche Scientifique, Paris 1965.
22. J. Demant and J. Wanklyn, *Corrosion*, **22**, 60 (1966).
23. A. MacRae, *Surface Sci.*, **1**, 319 (1964).
24. K. Lawless, F. Young, and A. Gwathmey, *J. Chim. Phys.*, **53**, 667 (1956).
25. B. Rose, *Phys. Rev.*, **44**, 585 (1933).
26. W. Brattain, *Rev. Modern Phys.*, **23**, 203 (1951).

The Chlorination Kinetics of Tungsten, Molybdenum, and their Alloys

A. Landsberg, C. L. Hoatson, and F. E. Block

Albany Metallurgy Research Center, Bureau of Mines, U. S. Department of the Interior, Albany, Oregon 97321

ABSTRACT

The chlorination kinetics of tungsten, molybdenum, and three of their binary alloys have been studied as part of a Bureau of Mines effort to provide information of value when considering chlorine metallurgy processes. Tungsten and molybdenum were used for this initial investigation of alloys because they are chemically similar, form a complete range of solid solutions, and have been shown to chlorinate at temperatures sufficiently different so as to facilitate the determination of temperature dependency of reactivity by experiments based on the measurement of weight loss as the volatile chlorides are formed. Both the pure metals and alloys containing 22, 48, and 72 atomic per cent (a/o) molybdenum were found to chlorinate between 400° and 775°C at rates of 10^{-7} to 10^{-5} mole per square centimeter per minute, with the reaction rate dependent upon the 0.6 power of chlorine pressure. Molybdenum exhibited the highest reactivity, tungsten was the least reactive, and the alloys showed intermediate reactivity with respect to temperature. Single crystals of the pure metals showed marked anisotropy upon chlorination. When chlorinated, the polycrystalline alloy specimens of 22 and 72% molybdenum tended to show the crystalline anisotropy exhibited by the major component, while the 48% molybdenum specimen developed no pattern similarity to the pure metals.

Chlorine reacts with all metals at appropriate temperatures and pressures. Some of the chloride products of such reactions volatilize at the temperatures at which detectable reaction occurs, leaving a clean metal surface during chlorination. Tungsten and molybdenum exhibit this characteristic. Their chlorination kinetics, studied previously in our laboratory (3), show a temperature difference of over 200°C for equal chlorination rates of the two pure metals. Simple removal of reaction products, a wide range of reaction

Key words: alloy chlorination, tungsten-molybdenum chlorination, molybdenum-tungsten chlorination, morphology of chlorination.

Table I. Spectrographic analysis of samples, ppm

Sample	Al	Ca	Cu	Fe	Mg	Mo	Ni	Si	Sn	Ti	W	Zr
W	5	20	1	5		100	5	500	5			
W-22 Mo	5	20	0.5	5			1	400	1	1		
W-48 Mo	5	10	0.5	5				200	5	1		
W-72 Mo	20		5	80	10		5	500	100			20
Mo	20			80	5			30			100	

No analysis was made for nonmetallic impurities.

temperatures, and the fact that these chemically similar metals form solid solutions in all proportions (2) suggest that the determination of temperature dependency of chlorination rate might be used conveniently for studying the effects of alloying on reactivity.

Experimental Work

Sample preparation.—The starting materials for the samples used in this study were metal powders supplied by the General Electric Company with average particle diameters of 3μ for the tungsten powder and 5μ for the molybdenum powder. Preweighed powders for each sample composition were mixed in a twin-V-shell blender for 15 min, passed through a 60-mesh screen, again mixed for 15 min, screened for a second time, and finally mixed for a third 15 min. Each blended composition was compacted isostatically, and the compacts were sintered in hydrogen at 2200°C for 10 hr. The resulting sintered bars of 90 to 95% of theoretical density were then consumable-arc-melted into ingots which were machined to a diameter of 1.5 in. and extruded at 1900°C to rectangular bars ⅜ x ¾ in. in cross section. These bars, after being conditioned by sand blasting to remove surface defects, were hot-rolled. A rolling temperature of 1450°C was used for the tungsten and the alloys, with a reduction of 20% per pass. The molybdenum was hot-rolled at 800°C, with a reduction schedule of 10% per pass. The final rolled thickness was 0.25 cm on all specimens. To reduce oxidation, all heating was done in an argon atmosphere. Sample specimens measuring 2.5 x 2.0 x 0.25 cm were machined from this rolled stock. Table I shows the impurity analysis for the samples used, and Table II shows the variation of sample composition from point to point as determined by an electron microprobe.

Single-crystal specimens were obtained from Materials Research Corporation. These materials were pure tungsten and molybdenum which contained no spectrographically detectable impurities. Crystal orientation was determined by x-ray reflection methods.

Table II. Typical electron microprobe analysis of sample surfaces*

Sample	Atomic per cent molybdenum			
	Before reaction		After reaction	
W-72 Mo	68.8		68.2	
	71.6		68.5	
	70.1		67.4	
	68.4		66.8	
	70.9		68.4	
	Average	70.0	Average	67.9
W-48 Mo	44.7		42.0	
	45.6		44.1	
	43.5		44.1	
	43.3		44.5	
	43.9		42.0	
	Average	44.2	Average	43.3
W-22 Mo	24.1		20.7	
	21.8		20.7	
	23.5		20.7	
	23.6		20.6	
	—		20.4	
	Average	23.2	Average	20.6

* These analyses were made randomly on highly polished sample surfaces with the electron beam of 1μ diameter to a depth of approximately 1000A. After reaction the surfaces were slightly roughened. Chemical analysis of large portions of the samples gave 22, 48, and 72 a/o molybdenum which reflect the composition changes in samples fabricated from the same ingot.

Procedure.—Chlorination-rate measurements were begun by weighing and measuring a metal sample. Weights were determined to the nearest 0.1 mg, and the rectangular measurements were made to the nearest 0.01 cm. The sample was then placed horizontally so that it rested slightly below center in a 28-mm Vycor[1] reaction tube which was held in a 3 x 30 cm tube furnace. C. P. grade argon and chlorine passing through control needle valves and calibrated rotameters were scrubbed in a bubbler containing sulfuric acid before entering the reaction tube. Gases leaving the reaction tube passed through another such bubbler and were vented via a laboratory hood. With the metal sample in place, argon was passed through the apparatus at the rate of 500 cc/min while the furnace was brought to operating temperature. The reaction-zone temperature was measured by a Chromel-Alumel thermocouple in a small Vycor tube positioned directly over the sample. After the reaction zone had been held at the desired operating temperature for several minutes, the reaction was started by substituting chlorine for part of the argon to give the desired chlorine concentration at a total gas flow of 500 cc/min. All work was done at 20% chlorine (approximately 152 Torr) except where noted. Reaction times ran from 15 min to 1 hr, during which the temperature remained constant to within ±2°C, and the gas flows were held to within 2% of the desired values. At the end of a run the chlorine flow was stopped and the argon flow increased while the entire reaction tube was cooled. When cool, the sample was removed and weighed. The weight loss was used to calculate the rate of reaction as moles of metal per minute per cm^2 of surface based on the geometric area and the average tungsten-molybdenum composition of the sample.

Results

The measured rates of chlorination, as moles of metal/cm^2 min, are shown graphically in Fig. 1. Data for each of the metal compositions given by open, filled, and partially filled symbols represent the experimental results from the three samples of each metal composition. Also each data point is the average of at least three replicate runs using an individual sample. The data show reproducibility from sample to sample, and the lines derived from a least squares analysis of the data according to the Arrhenius relationship agree quite well with our previous work on commercially prepared sheets of the pure metals. The least squares analyses are given in Table III. All samples changed in appearance as chlorination proceeded. Initially the surfaces appeared dull because of their sandblasted finish but became shiny as they reacted. The reaction rates increased during the two or three initial reaction experiments and then remained constant for an extended period of chlorination during which the experiments were made for the reported data. After the constant rate period of chlorination the samples were rough on all surfaces and very jagged on the edges in the direction of rolling and the reaction rate decreased slightly. These decreasing-rate data are not reported here. The composition of the sample sur-

[1] Reference to trade names is made to facilitate understanding and does not imply endorsement by the Bureau of Mines.

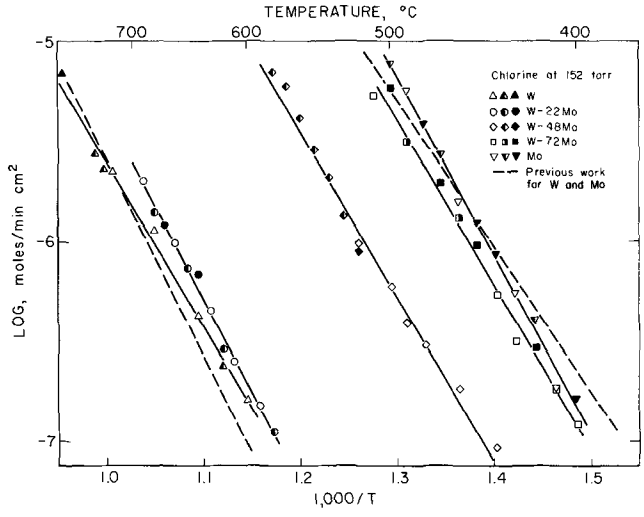

Fig. 1. Arrhenius plot for W-Mo chlorination

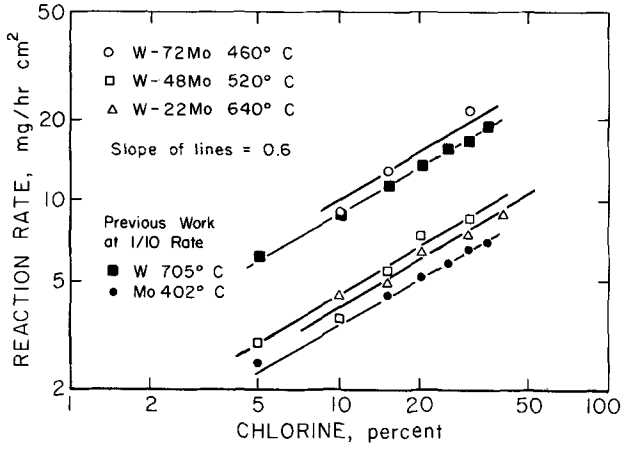

Fig. 2. Effect of chlorine pressure on reaction rate

faces showed slight preferential loss of molybdenum upon chlorination, as indicated by the electron microprobe measurements in Table II. The data, although presented in the table in pairs of analyses for before and after reaction, do not necessarily represent exactly the same location on the surface before and after reacting. These surfaces were only slightly reacted before the final microprobe analyses were made. Other tests in which over half of the entire sample was removed by chlorination showed no depletion of molybdenum. The resulting, very rough surfaces hindered accurate microprobe analyses.

The effect of chlorine pressure on the reaction rate is shown in Fig. 2. As in our previous work with the pure metals, the alloys showed a rate of chlorination

Table III. Least square equations for chlorination rates

Material	A*	B*
W	8254	2.65
W-72 Mo	9350	4.00
W-48 Mo	8295	4.51
W-22 Mo	8322	5.44
Mo	8961	6.48

* Constants for the equation

$$\log R = -\frac{A}{T} + B$$

where R is the chlorination rate in moles per cm² min with 20% chlorine and T is the absolute temperature in °K.

approximately dependent upon the 0.6 power of chlorine concentration. At the highest rates of chlorination measured, changes of total gas flow rates from 500 to 1000 cc/min produced no change in measured chlorination rates demonstrating that true chemical reaction was the rate-limiting factor.

Upon chlorination all samples changed in appearance because of the anisotropic attack of chlorine. The polycrystalline metals and alloys developed ridges and troughs running in the direction in which the samples had been hot-rolled. Figure 3 shows the trimmed ends of the molybdenum sample before and after chlorination. Interestingly, a sample which had been reacted at 1200°C did not develop the deep ridges and troughs but remained rather smooth with the individual grains becoming very evident. Microscopic views of these reacted samples are not of high quality because of the deep etching and low depth of field at high magnification. Nevertheless, in Fig. 4 these views do reveal a similarity between the reacted textures of tungsten and tungsten-22 molybdenum, and between molybdenum and tungsten-72 molybdenum with the tungsten-48 molybdenum texture being distinct. The molybdenum after chlorination at higher temperatures shows

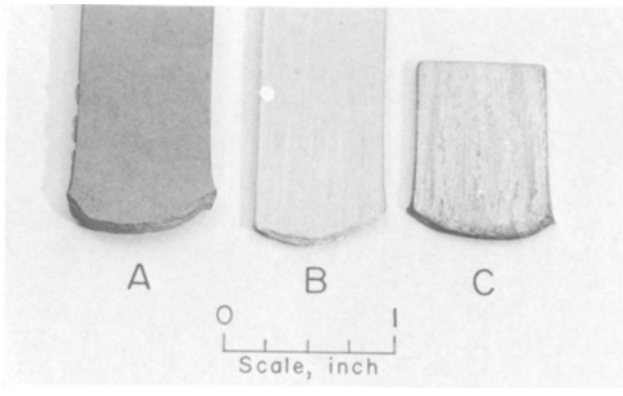

Fig. 3. Polycrystalline molybdenum samples. A is an unreacted molybdenum strip, B had been reacted at 480°C with 20% chlorine, and C had been reacted at 1200°C with 20% chlorine.

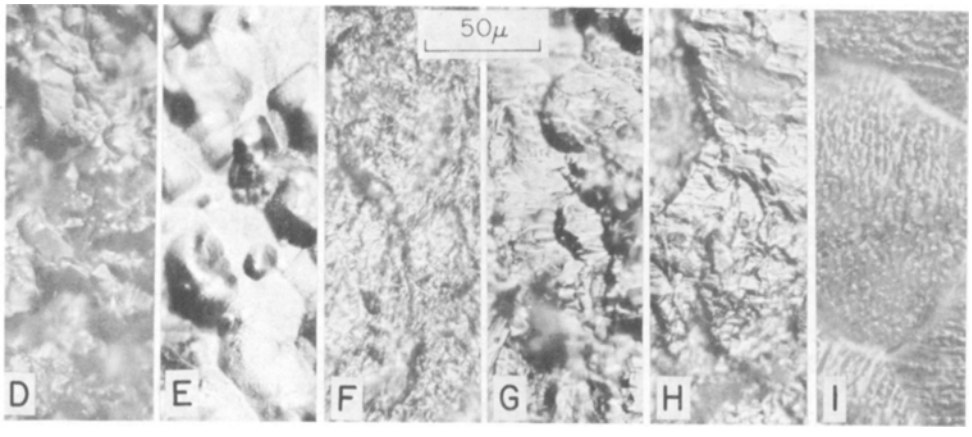

Fig. 4. Photomicrographs of chlorinated polycrystalline samples. D. Tungsten, 700°C., E. W-22 Mo, 700°C., F. W-48 Mo, 580°C., G. W-72 Mo, 480°C., H. Molybdenum 480°C., I. Molybdenum, 1200°C. Direction of rolling ↕.

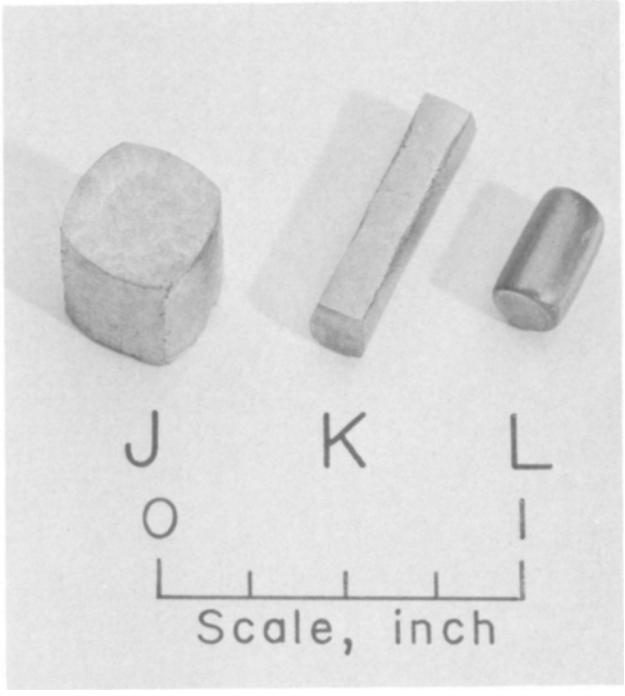

Fig. 5. Single-crystal specimens after chlorination. J. Tungsten, 700°C., K. Tungsten, 700°C., L. Molybdenum, 1200°C.

reaction produced rows of small circles running in different directions on adjacent crystals. This produces crystal differentiation on a macroscopic scale.

Single crystal samples show the anisotropic attack of chlorine quite clearly. Figure 5 is a photograph of two tungsten single crystals which have been extensively chlorinated at 700°C and a molybdenum crystal chlorinated at 1200°C. These specimens were cylindrical before reaction occurred. Because of the high reaction rate of molybdenum at 1200°C, gaseous diffusion limited the reaction rate, causing the somewhat rounded corners on the single crystal; however, close examination shows distinctive surface characteristics at 90° intervals. Electron microscope views in Fig. 6 of a molybdenum single crystal show surfaces in the early stages of attack by chlorine, and Fig. 7 and 8 show surfaces parallel or nearly parallel to the {100}, {110}, and {410} planes which have developed after extensive chlorination. Nomarski interference-contrast microscopic views of similar surfaces are shown in Fig. 9. Similar surface configuration resulted from chlorination at all chlorine concentrations and temperatures studied (except for the high-temperature experiments specifically noted).

Tungsten single-crystal surfaces developed similarly upon extensive chlorination. Two planar surfaces which formed on an originally cylindrical crystal were parallel to the {100} and {210} planes. Electron microscope

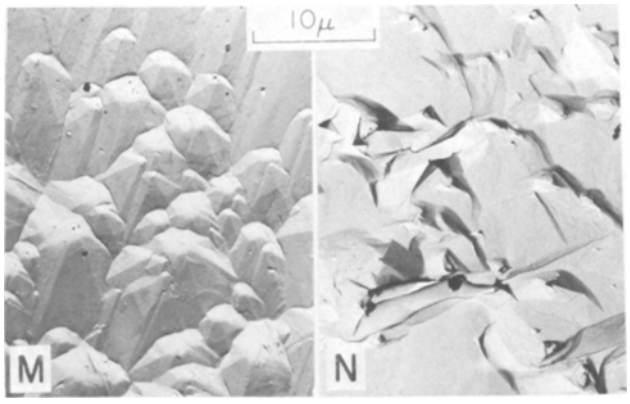

Fig 6. Electron micrographs of single-crystal molybdenum at the onset of chlorination. M. Reacting surface, N. Nonreacting area.

views of these surfaces are shown in Fig. 10. Optical microscope views of the surfaces which developed parallel to the {100}, {210}, and {320} planes are shown in Fig. 11.

The molybdenum crystal reacted with chlorine at 1200°C showed a series of microscopic rod-like depressions over the entire surface. These cylindrical pits were all parallel. Viewing the crystal microscopically from various angles revealed that the pit spacing varied periodically every 90° on surfaces parallel to their length, but perpendicular to their length the pits appeared as round holes in the metal surface.

Discussion

The chlorination of tungsten and molybdenum in the temperature range studied shows striking similarity to certain oxidation reactions of these metals. Perkins, Price and Crooks (5) have shown that within boundaries defined by temperature and oxygen pressure tungsten is oxidized without formation of an oxide scale at a rate proportional to the 0.59 power of the oxygen pressure. Single-crystal tungsten used by these investigators shows anisotropic attack by oxygen in this region. Other investigations (4, 7) have shown that oxygen attacks both tungsten and molybdenum with a similar fractional exponential dependence on oxygen pressure. Like the oxidation of these metals, the appearance of the chlorination-reaction-produced surfaces changes as the temperature rises. This was shown clearly for molybdenum chlorinated at 1200°C, the maximum temperature obtainable in our equipment (see Fig. 3 and 5). Tungsten surfaces chlorinated at 1200°C showed some dissimilarity to surfaces chlorinated at lower temperatures.

The marked anisotropy of the chlorination of tungsten and molybdenum as evidenced by the resulting morphology of single crystals demonstrates that certain crystal surfaces are reactive and also the fact that certain crystal planes are not chlorinated. This

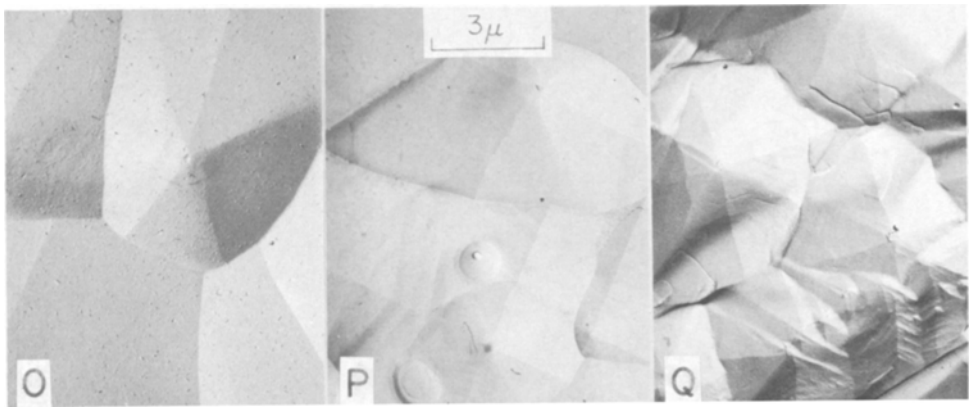

Fig. 7. Electron micrographs of chlorinated molybdenum single-crystal surfaces parallel to the {100} plane.

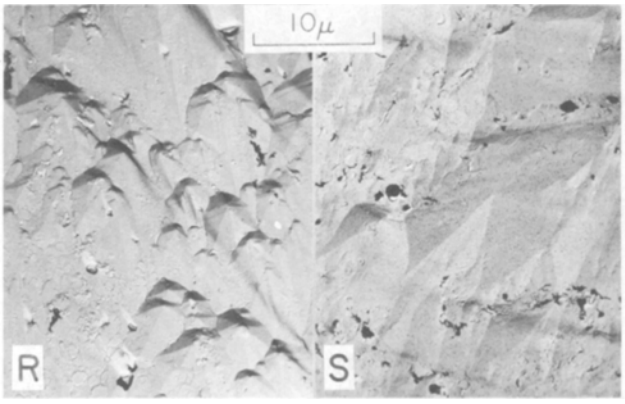

Fig. 8. Electron micrographs of chlorinated molybdenum single crystal surfaces. R is a {410} surface; S is a {110} surface.

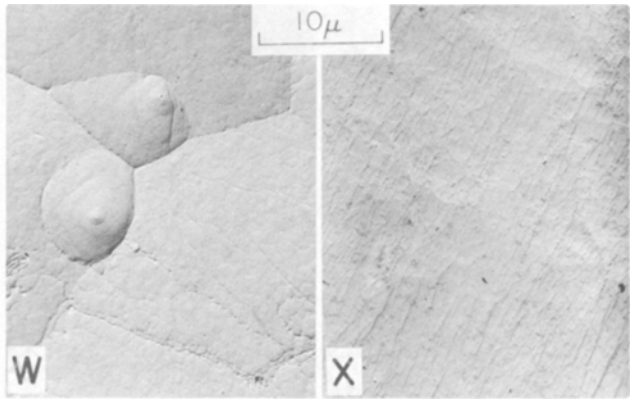

Fig. 10. Electron micrograph of chlorinated tungsten single-crystal surfaces. W is a {100} surface; X is a {210} surface.

is clearly shown in Fig. 5 by the very sharp corners on the reacted tungsten single crystals. Figure 6 also illustrates a contrast between the reactive and nonreactive faces of a single crystal. Even though the surfaces shown had only been exposed to chlorine for a few minutes, it is very clear that a marked pattern had already developed on one face while an adjacent area showed no change from the unreacted surface. Such areas alternated around the cylindrical crystal every 45°.

Examination of Fig. 7, 8, and 9 reveals a system of pyramids developed by chlorination on {100} molybdenum surfaces and surfaces close to {100}. The large surface area resulting from these pyramids (*e.g.* frame T) gives an indication as to why molybdenum upon chlorination recedes rapidly perpendicular to {100} planes. On some higher order planes similar pyramids appear slanted, and a pencillike structure is noted with the pyramid being in the sharpened-point position. A trisoctahedron form best correlates with the single-crystal morphology developed as the result of molybdenum chlorination.

Tungsten crystals also produce an octahedral form when chlorinated. The square pyramids shown in the electron photomicrograph of Fig. 10, W are severely rounded, but photomicrographs in Fig. 11 of the chlorinated {100} and {320} surfaces depict a sharper series of angular faces. The {210} faces, which reacted rather rapidly, show no clearly defined geometric pattern other than a series of shallow lines. The best geometrical shape that conforms to these chlorination-developed surfaces is a tetrahexahedron with faces made up of {210} planes.

From these tentative identifications of the reactive planes of tungsten and molybdenum, a difference in surface reactive geometry may be postulated for the two metals even though the over-all chemical mechanism may be similar. Indeed, this is observed in the chlorination-produced faceting under equal magnification and developed on materials which had a similar crystal texture due to rolling. [Reference (1) gives a rolled texture of (100) <011> for both tungsten and molybdenum.] The alloys rich in one metal develop a chlorination faceting similar to that of the pure metal and show a chlorination dependency on temperature similar to that of the high-content metal, but the alloy with nearly equal numbers of tungsten and molybdenum atoms develops a surface quite different from either of the pure metals. Dependency of chlorination rate on the nearly half power of the chlorine pressure may be attributed to the breakup of the chlorine molecule on the metal surface, and others (6) have shown that atomic chlorine is more reactive towards molybdenum; indeed it may be the only reactive chlorination species.

Positive identification of the reacting metal surfaces needs to be made, and a correlation between the various temperature-dependent regions of chlorination and the role of the metal surface must be determined before a complete understanding of the chlorination of tungsten and molybdenum and their binary alloys is realized. Such determinations would answer the question as to whether a certain crystal-oriented morphology develops on tungsten, molybdenum, and their alloys because of the atoms present or because of the temperature-chlorine pressure region of the reaction.

Manuscript submitted Dec. 23, 1970; revised manuscript received *ca.* March 25, 1971.

Any discussion of this paper will appear in a Discussion Section to be published in the June 1972 JOURNAL.

REFERENCES

1. C. S. Barrett and T. B. Massalski, "Structure of Metals," 3rd Edition, pp. 558-561, McGraw-Hill Publishing Co., New York (1966).
2. Max Hansen, "Constitution of Binary Alloys," 2nd

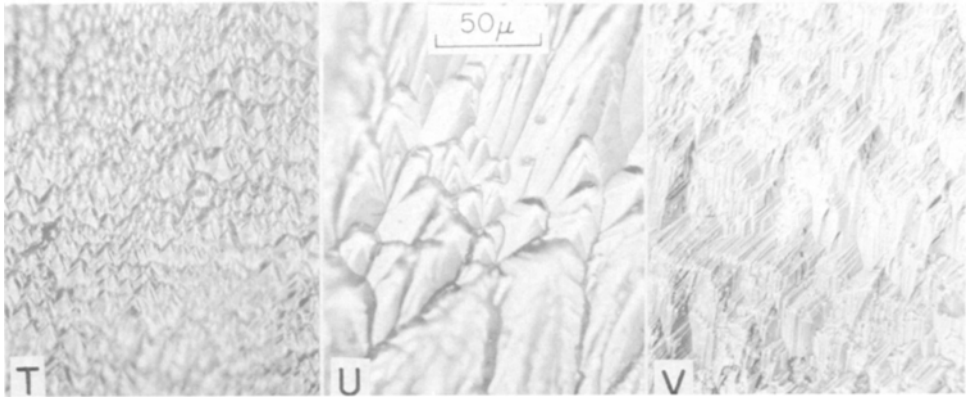

Fig. 9. Photomicrograph of chlorinated molybdenum single-crystal surfaces. T and U show {100} surfaces; V is a {110} surface.

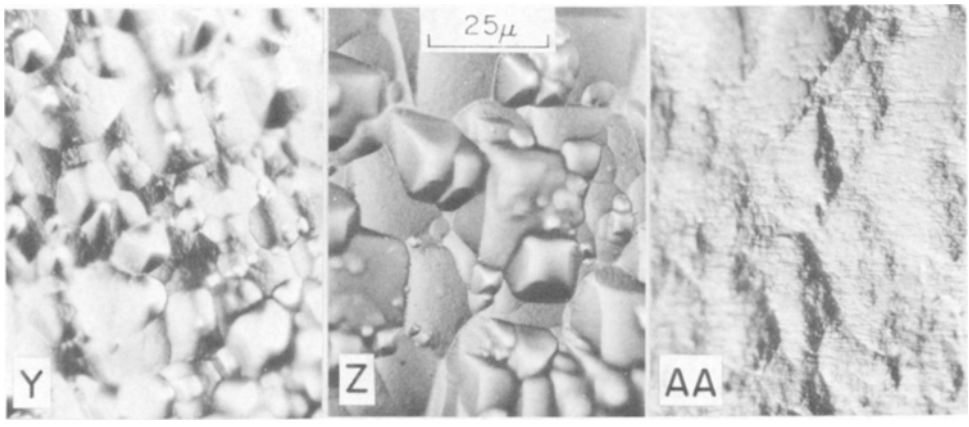

Fig. 11. Photomicrographs of chlorinated tungsten single-crystal surfaces. Y is a {100} surface; Z is a {320} surface; AA is a {210} surface.

Edition, p. 980, McGraw-Hill Publishing Co., New York (1958).
3. Arne Landsberg and F. E. Block, A Study of the Chlorination Kinetics of Germanium, Silicon, Iron, Tungsten, Molybdenum, Columbium, and Tantalum. *U. S. Bur. Mines, Rept. Invest.* 6649 (1965).
4. North American Aviation, Inc., Materials Research Department (Downey, Calif.) "High Temperature Oxidation of Molybdenum Under High Altitude Conditions." Rept. AL-2617, Sept. 1, 1957, ASTIA AD 147 839.
5. R. A. Perkins, W. L. Price, and D. D. Crooks, Oxidation of Tungsten and Other Refractory Metals, NASA Accession No. N66-13738, Report No. AFML-TR-64-162, April 1965.
6. D. E. Rosner and H. D. Allendorf, *J. Phys. Chem.*, **69**, 4290 (1965).
7. D. E. Rosner and H. D. Allendorf, *This Journal*, **114**, 305 (1967).

Mechanism of Sulfidation of Nickel-Chromium Alloys at 700°C as Inferred from Inert and Radioactive Marker Techniques

G. Romeo,*,[1] W. W. Smeltzer,* and J. S. Kirkaldy

Department of Metallurgy and Materials Science, McMaster University, Hamilton, Ontario, Canada

ABSTRACT

Sulfidation experiments have been carried out on a Ni-20 w/o Cr alloy using platinum markers and the tracer S^{35} to elucidate the transport mechanism for the diffusion-controlled formation of the duplex sulfide scale. It is concluded that outward diffusion of nickel and chromium accounts entirely for the growth of both layers. Chromium sulfide, being more stable than nickel sulfide, is formed by decomposition of the latter at the boundary between the two layers. This process is compensated for by a rapid growth of nickel sulfide at the gas-scale interface. It has been unequivocally demonstrated that sulfur diffusion does not contribute significantly to scale growth.

The results of a kinetic and morphological study of the scale formation on nickel-20 w/o (weight per cent) chromium alloys in hydrogen sulfide-hydrogen atmospheres were presented in an earlier publication (1). We report in this paper the results of a further series of experiments designed to elucidate the mechanism of the process. In particular, platinum markers and radioactive sulfur have been used to establish the contribution of the different species to the net transport of matter across the sulfide scale formed as a corrosion product. Such techniques have been widely employed in the past few years. We refer the reader to the papers by Mrowec and Werber (2-4) for further information and to an extensive and up-to-date bibliography on this subject in a recent paper by Holt and Himmel (5).

Experimental

Platinum marker experiments.—Specimens approximately 1.5 x 0.5 x 0.1 cm were cut from sheets of Ni-20 w/o Cr alloys. Details on composition and metallographical preparation prior to sulfidation have been reported in our earlier publication (1). In the same publication, the assembly was described for the concurrent sulfidation in hydrogen sulfide-hydrogen atmospheres of four specimens. The specimens could be raised to a relatively cold zone of the assembly and quenched after different reaction times. All experiments were carried out at 700°C which, as discussed in the previous work, was convenient for avoidance of the formation of a liquid phase. H_2S/H_2 atmospheres were used that ranged from 5 to 60 v/o (volume per cent) in hydrogen sulfide it being previously established that the pressure of sulfur has a negligible effect on the reaction mechanism.

Short pieces of 50μ diameter platinum wire were stretched across the surface of the specimens and electrically spot welded at several points and to the edges. Satisfactory adhesion to the surface of most markers was attained and the specimens could be sulfidized in the upright position. During later examinations of scale cross sections comparison of the relative positions of

* Electrochemical Society Active Member.
[1] Present address: Physical Chemistry Laboratory, General Electric Research and Development Center, Schenectady, New York 12301.
Key words: sulfidation, nickel-chromium, markers.